International Journal of Thermophysics, Vol. 7, No. 1, 1986

High-Pressure, High-Temperature Thermophysical Measurements on Tantalum and Tungsten[1]

A. Berthault,[2] L. Arles,[2] and J. Matricon[3]

A submillisecond resistive heating technique under high pressure (0.2 GPa) has been applied to the measurement of thermophysical properties of tantalum and tungsten metals in the solid and the liquid state. Agreement between previously published and most of the present results is good.

KEY WORDS: high pressure; high temperature; liquid metals; pulse method; tantalum; tungsten.

1. INTRODUCTION

Conventional static techniques for measuring thermophysical properties of materials are temperature and pressure limited by severe problems such as sample reactivity, evaporation, strength of the pressure vessel, and thermal losses at elevated temperatures. These problems are created by the exposure of the specimen and its immediate environment to high temperatures for long periods of time (more than 1 s).

High-speed techniques permit the elimination of most of these difficulties. The subsecond experiments of Cezairliyan et al. [1] are still much too slow to prevent the specimen, once in the liquid state, from collapsing under gravity and this technique is thus limited to solid metals. Submillisecond resistive heating techniques have been applied successfully to the measurement of thermophysical properties of liquid metals by Lebedev et al. [2], Shaner et al. [3], and Seydel and Fucke [4]. With a heating rate

[1] Paper presented at the Ninth Symposium on Thermophysical Properties, June 24–27, 1985, Boulder, Colorado, U.S.A.

[2] Commissariat à l'Energie Atomique, Boite Postale 511, Paris cedex 15, France.

[3] Groupe de Physique du Solide, Université Paris VII, 2 place Jussieu, 75251 Paris cedex 05, France.

0195-928X/86/0100-0167$05.00/0

840/7/1-12

of about 10^8 K · s^{-1}, radiative heat losses from the sample are reduced to a negligible level during the entire experiment, and the specimen continually remains in thermodynamical equilibrium.

The data published in this paper were obtained on liquid metals under a 0.2-GPa pressure and a temperature ranging from 1800 to 6000 K.

2. MATERIALS AND METHODS

The typical experimental procedure consists in resistively heating a wire-shaped sample in an argon gas-filled pressure cell while measuring the energy input, the volume expansion, and the temperature of the sample. Although the design pressure of this vessel is 0.9 GPa, we operated only up to 0.6 GPa. The bore of the cell is oriented vertically, the lower anvil containing the fill line and the upper anvil the electrodes. Both the pressure vessel and its anvils are placed inside a rectangular high-strength frame. Two lines of sight perpendicular to each other and to the axis of the bore enable observation of the sample.

2.1. Pressure

The actual pressure inside the sample is the sum of two terms: one is the gas pressure in the cell; the other is induced by the current flowing through the sample. The pressure due to the magnetic field in a wire carrying a uniform current is maximum along the axis and decreases parabolically to zero at the outermost radius of the conductor. The value of this pressure at the center of a wire sample 1 mm in diameter carrying a 20-kA uniform current is 0.04 GPa. The pressure in the cell is measured with a manganin gauge with an accuracy of ± 0.001 GPa. Due to the magnetic term, the actual value inside the sample during the pulse cannot be measured as accurately. The fact that all the measurements made at either 0.2 or 0.3 GPa on tantalum and tungsten give identical results shows that the maximum 0.04-GPa uncertainty is of no consequence for these materials.

2.2. Electrical Measurements

The energy deposition is accomplished by discharging a 60-kJ capacitor bank (20 kV, 300 μF) through the sample in about 100 μs. During this time, the radiative heat loss is negligible compared to the added electrical energy. No inhomogeneous heating results from the skin effect and the entire sample is always near thermodynamic equilibrium.

The value of the energy deposited is estimated from the running

integral of the current through the sample times the voltage drop across a known length of the wire. The inductive term, which is significant mainly during the rise time of the current, must be eliminated. An estimation is made using a constant value for the inductance and the measured time derivative of the current. The 9-nH value of the inductance used in our calculation is justified by the fact that the resulting resistive voltage shows no irrelevant variations, such as a sudden drop or negative value. We have established the fact that the error in the enthalpy introduced by a wrong inductance value never exceeds 0.1%, except during the first few microseconds of the experiment.

The current through the sample is recorded continuously through the inductive response of a Pearson probe which is accurate to within $\pm 0.5\%$ with a rise time of 200 ns and a drift of $0.002\%/\mu s$. The signals from the two voltage probes in contact with the sample are referenced to the ground potential of the Faraday cage which contains all the electronics. The signals are fed to a differential amplifier. A periodic calibration ensures an accuracy of $\pm 0.5\%$.

Current through the sample, voltage drop across the sample, and thermal emission from the sample are recorded with high-speed waveform recorders, each of them storing 2050 ten-bit words at a sampling rate of 0.1 μs. A master–slaves configuration eliminates any lag between the time bases of recorders. The precision of the time base is better than 0.1%. All the data are recorded with a precision of 0.1% (actually 1 part in 1024). The final accuracy of the current and voltage measurement is $\pm 0.6\%$. The sample length between the two voltage probes is estimated with an accuracy of $\pm 0.2\%$, the diameter of the wire with an accuracy of $\pm 1\%$, and the linear density with an accuracy of $\pm 0.1\%$. Except during the first few microseconds of the current pulse, where the inductive corrections are large compared to the resistive voltage, we can estimate the enthalpy to be accurate to $\pm 1.5\%$ and the resistivity to $\pm 4\%$.

2.3. Volume Expansion

The volume expansion is measured using an argon ion laser to provide permanent illumination for shadowgraph. The slit of a streak camera defines a given wire diameter, which is recorded continuously during the experiment. Since the two ends of the sample are blocked up by supporting jaws, only radial expansion is allowed and the specific volume varies with the square of the diameter. The accuracy in the diameter increment is $\pm 1\%$, giving the V/V_0 ratio with an accuracy of $\pm 2\%$, as long as the sample remains cylindrical during expansion. To check this requirement, a

snapshot of the whole frame is made at the end of the curent pulse using a Q-switched ruby laser for background lighting.

2.4. Temperature

The temperature measurement procedure is directly inspired from the multichannel pyrometric technique described by Gathers et al. [5]. The thermal emission of a rectangular (0.3×3-mm) portion of the wire is analyzed by four pyrometers tuned, respectively, at 900, 750, 600, and 450 nm through interference filters (100-nm bandwidth). The output curent of the photodiodes is logarithmically amplified and recorded on four waveform recorders. The main difficulty of the entire experiment resides in the actual evaluation of the temperature from the pyrometric data. Along the lines of Shaner et al. [6], we relate the output of the *ith* photodiode to temperature by

$$I_i(T) = G_i \int F_i(\lambda)\, D_i(\lambda)\, \varepsilon(\lambda, T)\, \frac{C}{\lambda^5 \exp(c/\lambda T - 1)}\, d\lambda$$

where G_i is an instrument factor including all kinds of losses along the optical path and the specific response of the photodiode, $\varepsilon(\lambda, T)$ is the wavelength-, teperature-, and surface-dependent emissivity of the sample. In the absence of any theoretical model, we assume ε to be temperature independent. The $F_i(\lambda)\, D_i(\lambda)$ product, which represents the spectral response of the filter F_i and the photodiode D_i, was measured separately.

Table I. Impurities in Tantalum and Tungsten Samples

	Composition (ppm weight)	
Impurity	Tantalum	Tungsten
Al	1.3	8
C	<20	15
Ca	0.13	12
Cr	0.8	12
Cu	0.4	<5
Fe	10	35
Mg	0.14	<10
Mo	1	60
N	45	10
Ni	11	<5
O	115	70
W	<1	

The calibration of the logarithmic amplifiers was achieved using the following procedure. The entire temperature range was simulated by illuminating the photodiodes with a laser beam attenuated through calibrated neutral-density filters. For each specimen, the response curve of each pyrometer was calibrated by assigning the melting plateau to the melting temperature estimated from the standard value corrected for the Clausius–Clapeyron term. This correction was calculated using our measured solid and liquid specific volumes and melting heat for the corresponding static pressures.

The recorded intensities at the tantalum melting point (3280 K) and the extrapolated emissivities of this metal at the wavelength of the four channels give set of values for the G's.

The C and c values are, respectively, 37412.6 $W \cdot \mu m^4 \cdot cm^{-2}$ and 14388 $\mu m \cdot K$.

3. RESULTS

3.1. Tantalum

The chemical purity of our sample is given in Table I.

The specific mass at 295 K is obtained by the fluid displacement method in a pycnometer. The 16.59 10^3 $kg \cdot m^{-3}$ figure obtained is in good agreement with the generally reported value of 16.6 10^3 $kg \cdot m^{-3}$.

The surface of the wire is reasonably free of defects and displays metallic brightness.

The electrical resistivity is measured during a low-power experiment before the final experiment. This experiment is low enough to prevent any significant heating of the sample. The resulting value is 14.7 10^{-8} $\Omega \cdot m$.

The characteristic features of the experiment reported here are given in Table II.

Table II. Characteristic Features of the Experiments Reported for Tantalum and Tungsten

	Tantalum	Tungsten
Argon pressure	0.2 GPa	0.2 GPa
Voltage of the Bank	13 kV	14 kV
Maximum current	18 kA	18.4 kA
Heating rate	10^8 $K \cdot s^{-1}$	3.5 10^7 $K \cdot s^{-1}$
Maximum temperature	6250 K	5500 K

Table III. Thermophysical Data for Tantalum [Enthalpies $H_s(T_m)$ and $H_l(T_m)$ Are Determined from the Curve of the Resistivity Versus Enthalpy]

H(MJ·kg^{-1})	T(K)	ρ (10^{-8} Ω·m)	V/V_0
0.30	2200	85.5	1.046
0.35	2490	94.5	1.057
0.40	2780	102.4	1.063
0.45	3040	109.5	1.073
0.496 (s)	3280	115.5	1.084
0.673 (l)	3280	134.0	1.138
0.75	3630	134.9	1.156
0.80	3870	136.2	1.166
0.85	4080	137.1	1.175
0.90	4330	137.9	1.189
0.95	4560	138.7	1.201
1.00	4790	139.9	1.214
1.05	5020	141.2	1.228
1.10	5250	143.0	1.243
1.15	5490	144.8	1.254
1.20	5710	146.6	1.270
1.25	5940	148.5	1.281
1.30	6180	150.7	1.300

Table III gives the smoothed values for the temperature, enthalpy, resistivity, and relative volume for the 0.2-GPa isobar.

The two electrical measurements (voltage and current) along with the volume measurement are not distorted by uncertain approximations. The resulting enthalpy, volume expansion, and resistivity may be safely calculated all along the experiment. The plot of V/V_0 and ρ versus enthalpy are shown in Fig. 1. Figure 2 shows the enthalpy plotted versus the temperature calculated from the data obtained with the 750-nm pyrometer. The two other pyrometers would have given exactly the same result. Figure 3 shows volume and resistivity versus the same temperature scale with references to literature values.

3.2. Tungsten

The surface of the sample was not as bright as that for the tantalum. A specific mass of 19.08 10^3 kg·m^{-3} at 295 K was obtained by the fluid displacement method.

The measured value for the electrical resistivity is 5.9 10^{-8} Ω·m. The characteristic features of the experiment reported here are given in Table II.

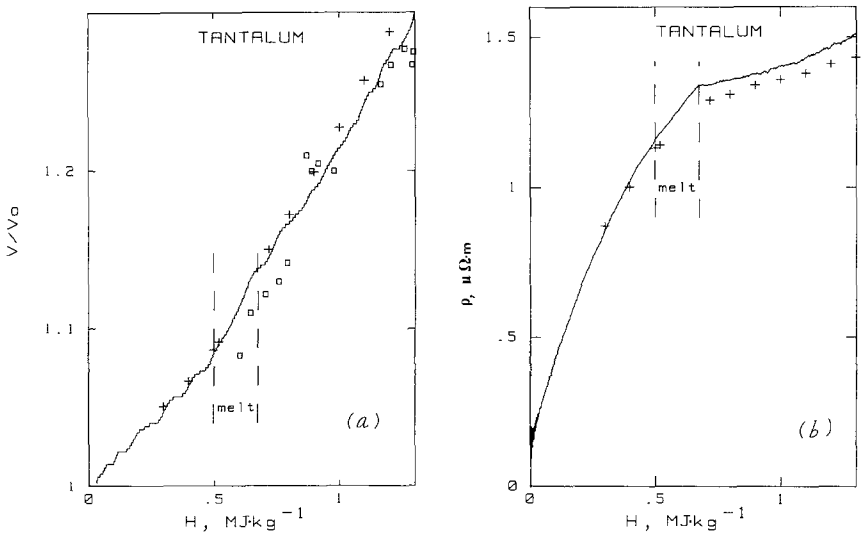

Fig. 1. Tantalum. (a) Relative volume of tantalum versus enthalpy at 0.2 GPa. (——) Our results; (+) Gathers [8]; (□) Ivanov et al. [15]. (b) Resistivity versus enthalpy. (——) Our results; (+) Gathers [8].

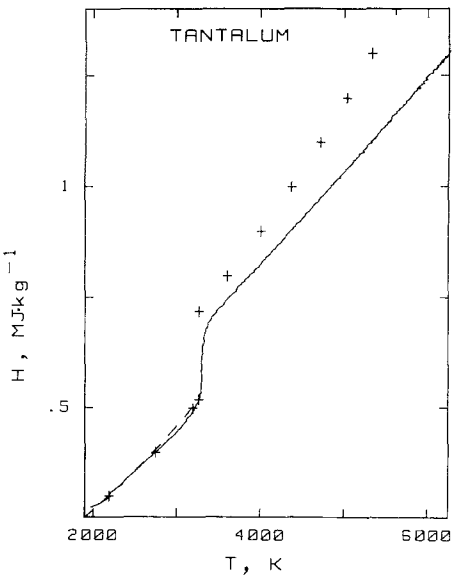

Fig. 2. Tantalum. Enthalpy versus temperature obtained by the 750-nm pyrometer. (——) Our results; (– – –) Cezairliyan et al. [1]; (+) Gathers [8].

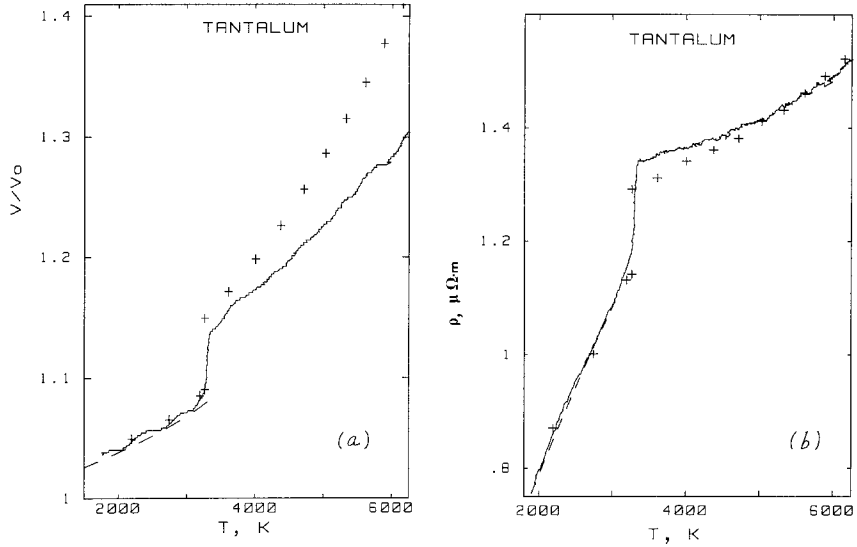

Fig. 3. Tantalum. (a) Relative volume of tantalum versus temperature. (——) Our results; (+) Gathers [8]; (– – –) Miiller and Cezairliyan [16]. (b) Resistivity versus temperature. (——) Our results; (+) Gathers [8]; (– – –) Cezairliyan et al. [1]. Note the discrepancy between our results and Gathers's data, which results from the discrepancy between the temperature scales above the melting point.

Table IV gives the smoothed values for the temperature, enthalpy, resistivity, and relative volume for the 0.2-GPa isobar.

Figures 4, 5, and 6 show, respectively, the evolution of the relative volume, the resistivity with an without expansion correction, and the enthalpy versus temperature.

4. DISCUSSION

Measurements similar to those reported in this paper have already been published by other authors and were obtained either by the submillisecond technique [2, 6–11, 19] or by quasi-static techniques [1, 12]. All the data are summarized in Table V for comparison.

4.1. Tantalum

Our expansion coefficient and resistivity (calculated by taking into account the thermal expansion) versus enthalpy (Fig. 1) are in good agreement with the results obtained with similar submillisecond techniques [8, 15].

Once expressed as a function of temperature, our data for the expan-

Table IV. Thermophysical Data for Tungsten

H (MJ · kg^{-1})	T (K)	ρ (10^{-8} Ω · m)	V/V_0
0.25	2010	58.6	1.044
0.30	2300	69.7	1.053
0.35	2560	80.1	1.062
0.40	2810	90.6	1.070
0.45	3060	99.6	1.088
0.50	3280	106.9	1.097
0.55	3460	113.9	1.097
0.60	3630	121.9	1.105
0.616 (s)	3690	123.2	1.108
0.87 (l)	3690	138.0	1.178
0.95	3840	138.0	1.196
1.00	4010	138.0	1.210
1.05	4180	138.0	1.223
1.10	4340	138.0	1.240
1.15	4510	138.0	1.254
1.20	4680	138.0	1.272
1.25	4840	138.0	1.290
1.30	5010	138.0	1.308
1.35	5180	138.0	1.328
1.40	5340	138.0	1.349

Table V. Some Thermophysical Data for Tantalum and Tungsten at Their Melting Temperatures (Values in Parentheses Were Published Without Thermal Expansion Correction)

Element	ΔH_{fus} (MJ·kg^{-1})	$\rho_s(T_m)$ ($\mu\Omega$·m)	$\rho_l(T_m)$ ($\mu\Omega$·m)	$V_s(T_m)$ (10^{-5} m^3·kg^{-1})	$V_l(T_m)$ (10^{-5} m^3·kg^{-1})	$C_p(T_m)$ (J·kg^{-1}·K^{-1})	Ref. No.
Ta	0.177	1.16	1.34	6.53	6.86	210	This work
	0.20	1.14	1.29	6.57	6.93	242	8
	0.23	1.00	1.15			245	10
	0.207	(1.19)	(1.31)				11
W	0.254	1.23	1.38	5.81	6.17	300	This work
	0.275	1.20	1.37		6.28	310	9
	0.250	1.18	1.32	5.84	6.15	282	6, 7
	0.299	(1.18)	(1.27)				2
	0.296	(1.15)	(1.25)				13

sion coefficient (Fig. 3a) and resistivity (Fig. 3b) in the solid state compare very well with the results of Miiller and Cezairliyan [16] and Cezairliyan et al. [1] obtained with subsecond techniques, although Cezairliyan's resistivity, calculated without a correction for thermal expansion, is slightly smaller than the results of our work. In the liquid phase our results depart from Gathers's, although they were obtained under similar experimental conditions, for the temperature estimate above the melting point (Fig. 2). Our value of $210\,J \cdot kg^{-1} \cdot K^{-1}$ for the constant-pressure heat capacity of the liquid phase is in good agreement with the values given by Gallob et al. [9] ($245\,J \cdot kg^{-1} \cdot K^{-1}$) and Gathers [8] ($242\,J \cdot Kg^{-1} \cdot K^{-1}$) at the melting point, but the different temperature scales above T_m result in a different temperature dependence of the relative volume (Fig. 3a), the resistivity (Fig. 3b), and the heat capacity (Fig. 2). For example, the relative volume expansion coefficient and the heat capacity, which are constant in our data over the whole temperature range of our measurements (3280 to 6250 K), vary linearly with temperature in Gathers's results.

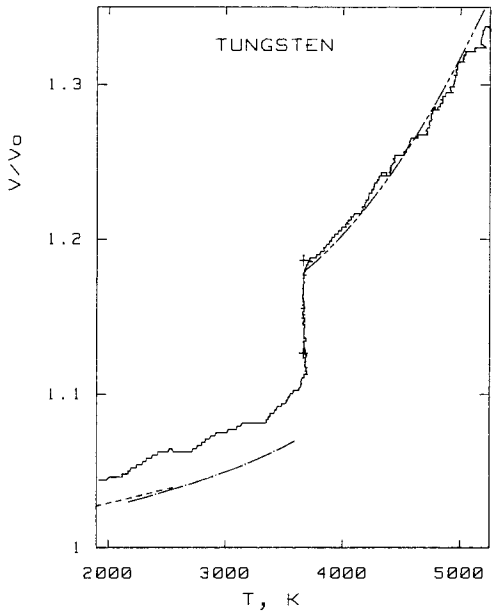

Fig. 4. Tungsten. Relative volume of tungsten versus temperature at 0.2 GPa. (——) Our result; (– – – –) Waseda and Ohtani [17]; (–· – ·–) Petukhov and Chekhovkoi [18]]; (– ··–··–) Seydel and Kitzel [19].

4.2. Tungsten

Our thermal expansion coefficient for the solid phase in the range 1900–3600 K is almost the same as the average value obtained by quasi-static techniques (Fig. 4) [17, 18], although the specific volume of the solid at T_m, in good agreement with the figure given by Shaner et al. [7], is 30% larger than the extrapolated static value. Along the lines of Dikhter and Lebedev [14], one may assume that during the fast heating process, relatively unstable defects (for example, Frenkel defects) which produce an anomalous thermal expansion are created. The agreement is excellent with the results of Seydel and Kitzel [19] in the liquid phase and Shaner et al. [7] at the melting temperature.

Concerning the resistivity, the comparison is difficult because the process of volume expansion is different in the fast and the slow heating techniques: during quasi-static heating, the sample is free to expand radially as well as axially; however, in fast heating only radial expansion is possible. The voltage drop is measured between two probes which follow the sample expansion in the quasi-static case but are at rest in the dynamic case. Without any expansion correction, our resistivity (Fig. 5a) in the solid

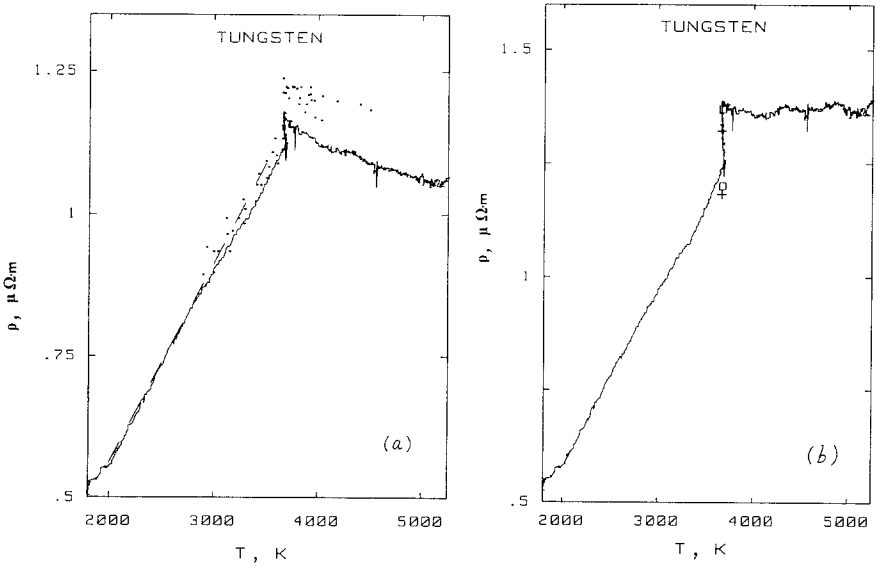

Fig. 5. Tungsten. (a) Resistivity versus temperature without any expansion correction. (——) Our results; (– – –) Cezairliyan and McClure [12]; (·) Dikhter and Lebedev [14]. (b) Resistivity versus temperature corrected for thermal expansion. (——) Our results; (+) Shaner et al. [7]; (□) Seydel et al. [9].

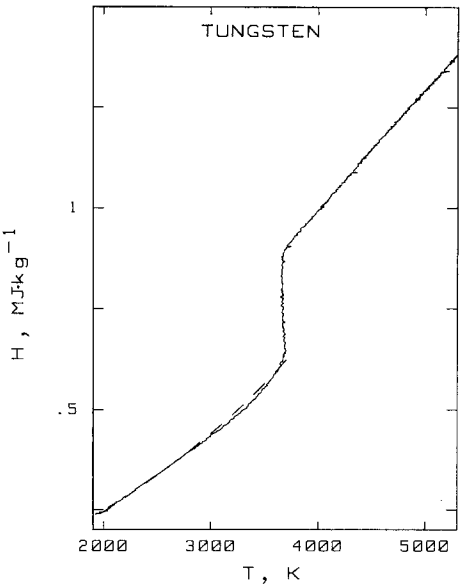

Fig. 6. Tungsten. Enthalpy versus temperature at 0.2 GPa. (——) Our results; (– – – –) Cezairliyan and McClure [12].

phase agrees fairly well with that of Dikhter and Lebedev [14] but is, as expected, smaller than Cezairliyan's value. In the liquid state, our data agree reasonably well with the values of Dikhter and Lebedev [14]. Figure 5b shows the resistivity corrected for thermal expansion. Note the plateau in the liquid state and the good agreement with the results of Seydel et al. [9] and Shaner et al. [7].

Figure 6 and the excellent agreement of our constant-pressure heat capacity with previous results (Table V) show that our thermometric scale is in total accordance with the other published data [6, 9, 12]. Under these conditions, the discrepancy observed for tantalum is difficult to understand.

REFERENCES

1. A. Cezairliyan, J. L. McClure, and C. W. Beckett, *J. Res. Natl. Bur. Stand.* **75A**:1 (1971).
2. S. V. Levedev, A. I. Savvatimskii, and Yu. B. Smirnov, *High Temp. (USSR)* **9**:578 (1971).
3. J. W. Shaner, G. R. Gathers, and C. Minichino, *High Temp. High Press.* **9**:331 (1977).
4. U. Seydel and W. Fucke, *Z. Naturf. Teil.* **32A**:994 (1977).
5. G. R. Gathers, J. W. Shaner, and R. L. Brier, *Rev. Sci. Instrum.* **47**:471 (1976).
6. J. W. Shaner, G. R. Gathers, and W. M. Hodgson, in *Proceedings of the Seventh Symposium on Thermophysical Properties*, A. Cezairliyan, ed. (ASME, New York, 1977), p. 896.

7. J. W. Shaner, G. R. Gathers, and C. Minichino, *High Temp. High Press.* **8**:425 (1976).
8. G. R. Gathers, *Int. J. Thermophys.* **4**:149 (1983).
9. U. Seydel, H. Bauhof, W. Fucke, and H. Wadle, *High Temp. High Press.* **11**:635 (1979).
10. R. Gallob, H. Jäger, and G. Pottlacher, *High Temp. High Press.* **17**:207 (1985).
11. S. V. Lebedev and G. I. Mozharov, *High Temp. (USSR)* **14**:1132 (1976).
12. A. Cezairliyan and J. L. McClure, *J. Res. Natl. Bur. Stand.* **75A**:283 (1971).
13. M. M. Martynyuk, I. Karimkhodzhaev, and V. I. Tsapkov, *Sov. Phys. Tech. Phys.* **19**:1458 (1975).
14. I. Ya. Dikhter and S. V. Lebedev, *High Temp. (USSR)* **9**:845 (1971).
15. V. V. Ivanov, S. V. Lebedev, and A. I. Savvatimskii, *J. Phys. F Met. Phys.* **14**:1641 (1984).
16. A. P. Miiller and A. Cezairliyan, *Int. J. Thermophys.* **3**:259 (1983).
17. Y. Waseda and K. H. Ohtani, *High Temp. High Press.* **7**:221 (1975).
18. V. A. Petukhov and V. Ya. Chekhovskoi, *High Temp. High Press.* **4**:671 (1972).
19. U. Seydel and W. Kitzel, *J. Phys. F Met. Phys.* **9**:L153 (1979).